

Extended cellular automaton models of solar flare occurrence

K.P. Macpherson¹ and A.L. MacKinnon²

¹ Department of Physics (Theoretical Physics), Oxford University, 1 Keble Road, Oxford OX1 3NP, UK (kpm@thphys.ox.ac.uk)

² Department of Adult and Continuing Education, University of Glasgow, Glasgow G12 8QQ, UK (alec@astro.gla.ac.uk)

Received 13 August 1998 / Accepted 31 August 1999

Abstract. In a previous study, we proposed a class of stochastic cellular automaton models for the occurrence of solar flares. ‘Flaring elements’ of a deliberately unspecified nature were allowed to interact. Investigation of a 1-D version of the model, capable of analytical description, conflicted in detail with observations but indicated the qualitative success of such a picture. In this extended study, we investigate the consequences of relaxing various assumptions present in the initial study. In this way we can build up a family of models each producing a better match with the observations. From these results we can say which features control the power-law indices obtained from self-organising models of flare occurrence. The sorts of constraints this type of modelling produces will also have to be satisfied by more physically detailed pictures.

Key words: Sun: activity – Sun: flares – Sun: magnetic fields – Sun: X-rays, gamma rays

1. Introduction

Detailed studies of individual solar flares have led to many advances in our understanding of these explosive events. Very large events, for instance, display the extremes of which the flare energy release process is capable, and thus place the greatest demands on theoretical models. Other, perhaps lesser events are fortuitously well-observed across a range of wavelengths and help to provide a picture of - one hopes - the ‘typical’ flare. However, statistical studies of very many flares offer another angle on flare energy release, and provide data on the distribution of flare parameters which a complete theory of flare energy storage and release must be able to address. In particular, hard X-ray observations are believed to yield a very direct measure of the primary flare energy (e.g. MacKinnon 1986), and high-quality data sets from recent spacecraft missions have yielded frequency distributions of various gross flare parameters, as viewed in this wavelength range.

In particular, Dennis (1985) and Crosby et al. (1993) studied X-ray data from the Solar Maximum Mission’s Hard X-Ray Burst Spectrometer (SMM HXRBS) to show that the flare frequency distribution as a function of energy is described by a

power-law over the observed range of 10^{27} to 10^{33} ergs (total energy in fast electrons inferred on the assumption of a thick target bremsstrahlung interpretation of the X-rays). Power-law functional forms are also obtained when constructing frequency distributions for flare duration and peak flux. Other recent studies of ISEE 3/ICE X-ray data (Lee et al. 1993), Compton Gamma Ray Observatory BATSE data (Biesecker 1994) and Yohkoh Soft X-ray Telescope data (Shimizu 1995) have all obtained power-law distributions for flare frequency distributions, with consistent power-law indices. The last of these reflects thermal flare plasma, rather than accelerated, nonthermal particles, and thus reassures us that hard X-rays are indeed related to total flare energy.

All of these power-law frequency distributions indicate that solar flares behave identically over all the size scales so far observed. Further supporting evidence for this comes from recent studies of solar radio noise storms in which the peak flux density of type I radio bursts has also been found to be well represented by a power-law distribution (Mercier & Trotter 1997). Krucker & Benz (1998) have used the EUV Imaging Telescope onboard the Solar and Heliospheric Observatory (SOHO) to observe heating events in the range 8×10^{24} to 1.6×10^{26} ergs, which appear to follow a power-law frequency distribution in energy, with a power-law index between 2.3 and 2.6, although see also Berghmans et al. (1998) who calculate a different index as a result of using different event selection criteria. These events may prove to be just scaled down versions of the larger flares which have been observed for years.

Several models have been developed to try and account for the power-law distributions observed (Rosner & Vaiana 1978; Lu & Hamilton 1991 - hereafter LH; Lu et al. 1993; Zirker & Cleveland 1993; Litvinenko 1996; MacKinnon et al. 1996; Wheatland & Glukhov 1998; Georgoulis & Vlahos 1996, 1998). In particular, LH seized on the concept of self-organised criticality (SOC - Bak et al., 1987, 1988) to introduce a new way of looking at solar active region evolution. SOC arises in driven, dynamical systems as a result of competition between two factors: the external driver of the system; and the internal rearrangement which occurs when the system state locally exceeds some critical threshold. The dynamics of sandpile avalanches give the canonical example of such a system (Bak et al., 1987, 1988), but other examples abound across the natural sciences,

Send offprint requests to: K.P. Macpherson

for instance: earthquake dynamics (Carlson & Langer 1989), cloud formation (Nagel & Raschke 1992) and grasshopper infestations in the American Midwest (Lockwood & Lockwood 1997). In the picture of LH, later developed in Lu et al. (1993) and Lu (1995a, b), the external driving comes from the convection zone velocity field, twisting and braiding the magnetic field lines in the corona until the field gradient locally becomes great enough for the field connectivity to change suddenly, releasing energy, in reconnection.

SOC simulations of ‘flare’ avalanche behaviour have suggested that the size distribution will be close to that observed for actual solar flares (LH; Lu et al. 1993; Vlahos et al. 1995; Galsgaard 1996). Indeed some of the initial results seemed to suggest power-law distributions similar to those observed were obtained almost independently of the details of the simulations. Georgoulis & Vlahos (1996, 1998) have, however, demonstrated how changing the rules governing the internal rearrangement of the field within a LH-type model can affect the power-law indices of the distributions (see also Galsgaard, 1996). Thus the details of the LH-type SOC model may have to be tailored in a slightly unsatisfactory way to reproduce observations.

In a previous work (MacKinnon et al. 1996 - hereafter Paper I), we succeeded in producing a power-law event size distribution using a very simple, statistical model. We wanted to explore, in as model-independent a way as possible, how far the observed flare distribution could be interpreted as an ‘avalanche’, as opposed to a ‘fragmentation’. In view of the state of understanding of 3-D reconnection, and certain comments about dimensionality, aired particularly by Wheatland & Sturrock (1996), the physical justification for the specifics of the LH approach is slender. Hence our ‘general’ idea is simply that of ‘avalanche’; and our approach attempts to take that general idea, in simple, Markov chain form, see how far observations appear to be consistent with it, and consequently derive very general constraints.

We arrange ‘elementary’ energy release events on a grid and allow them to trigger one another, according to the rules below, in energy release ‘avalanches’. The physical nature of the elementary energy release events is deliberately unspecified, since various candidates exist. Without assuming any particular physical interpretation, we might suppose that they correspond to the X-ray, radio and UV ‘microflares’ or ‘transients’ observed in active regions (Lin et al. 1984; Bastian 1991; Shimizu et al. 1992; Gopalswamy et al. 1994; White et al. 1995; Porter et al. 1995; Gary et al. 1997). The probability of energy release at any one location on the grid depends only on whether energy release has taken place at the neighbouring locations. Thus no grand organising principle is necessary to obtain events of arbitrary size, only the ‘self-organisation’ of elementary energy release events.

In Paper I we concentrated on a very simple, one-dimensional cellular automaton (CA) model in which each energy release site has two neighbours. Certain simplifying assumptions combined to yield a situation which: could be described completely analytically; sufficed to make the qualitative points above; and provided a useful comparison with the

‘self-organised critical’ models. The model yielded a power-law event size distribution not in direct agreement with observations, but we gave a plausibility argument that relaxing any of the simplifying assumptions of the model could bring this index into closer agreement with observations. In Macpherson & MacKinnon (1997 - hereafter Paper II) we explored the parallels between our model construction and percolation models for co-operative phenomena, in particular relaxing one of our initial assumptions to generate a new class of percolation model for transient phenomena. Litvinenko (1998) has applied methods of branching theory to our model as described in Paper II to derive asymptotic estimates for the power-law event size distribution, independent of the dimensionality of the model. In the present work we further explore the parallels with percolation theory, re-assessing the significance of Paper II’s results for flare studies, and considering cases with more than one dimension. In particular we wish to see how far the plausibility argument of Paper I can be rigorously justified. We anticipate finding constraints on the connectivity and/or intrinsic timescales characterising elementary energy release events in this process.

The structure of this paper is as follows: in the following section we review briefly the analytical results of Paper I and the numerical simulations carried out in Paper II which are shown to agree with, and extend, the analytical treatment. In particular, since Paper II concentrated purely on the dynamics of our extended model, we re-assess these results for the context of solar flares. In Sect. 3 we extend the model into 3 dimensions. We find that all of these further developments produce models intractable, as yet, to detailed analytical study and so rely on Monte Carlo type simulations of their behaviour. Finally, in Sect. 4 we discuss our results and methodology in context with alternative statistical models of flare occurrence and in Sect. 5 present the conclusions which this work leads us to.

2. Review of the basic model

Paper I modelled the idea that elementary energy releases may self-organise to produce large events using a stochastic cellular automaton approach, consisting of an assembly of potential energy release sites, on a discrete (space, time) lattice. The triggering rules of Paper I are summarised as follows. An inactive site can become active with probability p_1 if one of its neighbours is active in the previous timestep. The site remains active for one timestep, with no repeated activation of any site within the same event allowed. At time $t = 0$, there is one active site and the model evolves thereafter according to the rules specified. We call an ‘event’ a sequence of temporally and spatially connected active sites, and the ‘size’ of an event the total number of elementary energy releases (ie active sites) involved in the event.

In this simple, 1-D case, event probabilities may be enumerated exactly, for fixed p_1 (Paper I). There are N distinct ways of getting an event of size N , each with probability

$$p_1^{(N-1)} (1 - p_1)^2 \quad (1)$$

The $(1 - p_1)^2$ factor is necessary to make the flare stop when it reaches size N ; its exponent results simply from the 1-D geometry. Thus the total probability of getting an event of size N is

$$P(N) = N p_1^{(N-1)} (1 - p_1)^2 \quad (2)$$

Acknowledging that p_1 will vary with time and place, we treat it as a random variable and average Eq. (2) over p_1 to get

$$\bar{P}(N) = \int_0^1 P(N) dp_1 \sim N^{-2} \quad \text{as } N \rightarrow \infty \quad (3)$$

in agreement with the form, if not the detail of observations.

We denote by $\eta(N)$ the number of distinct ways in which an event of size N can occur. In the 1-D case of Paper I, $\eta(N) = N$.

Various natural extensions of Paper I's simple construction are possible. The argument leading to Eqs. (2) and (3) suggests that any such extensions resulting in $\eta(N) \sim N^{1.5}$ would produce $\bar{P}(N)$ in good agreement with observations. Indeed Litvinenko (1998) uses asymptotic results of branching theory to show $\eta(N) \sim N^{1.5}$ for any system of dimensionality greater than one.

In Paper I we suggested that we might obtain more detailed agreement with observations by increasing the number of ways of getting an event of size N . We proposed that considering dimensions greater than one, and/or allowing for the repeated activation of lattice sites within one event, as natural extensions to the basic model. We note that repeated activation is an existing property of the LH formulation and, moreover, that flare energy release is often observed to occur locally within the flaring timescale. In Paper II, we thus considered the dynamical behaviour resulting from the removal of the restriction of no repeated flaring. This was achieved by introducing p_{re} , the probability for a site to become active again subsequent to flaring once.

The model of Paper I, and its natural extensions into 2-D and 3-D are identical with those of percolation theory - the causal element of the present work does not affect the mathematical structures - with our events identical to percolation clusters. In addition, in Paper II we demonstrated that the dynamical behaviour of the model with repeated activation allowed can be regarded as a form of directed percolation in two (one space + time) dimensions. Percolation theory (e.g. Stauffer & Aharony 1994) teaches us to expect: an absence of exact analytical results in all but the simplest cases (Paper I); and that arbitrarily large events may occur for $p_1 > p_c$, a critical probability whose exact value is determined by the dimensionality, etc. of the model. In 1-D, $p_c = 1$.

As an example, Fig. 1 (from Paper II) shows the dependence of mean event size on p_1 , for several values of p_{re} . We note the occurrence of $p_c < 1$ for any value of $p_{re} > 0$. The solid line corresponds to the limit of $p_{re} = 0$, namely Paper I, where the mean event size can be shown to have the functional form $\langle N \rangle = (1 + p_1)/(1 - p_1)$.

2.1. Paper II's results reassessed for flare studies

Employing Monte Carlo-type simulations, we demonstrated in Paper II that event size distributions in good agreement with observations can be obtained, in the limit $p_{re} \rightarrow 1$, i.e. in the limit that sites re-attain flaring potential after only one timestep. Of course, to obtain such a result, p_1 had to be restricted to the range $p_1 < p_c$. Assume for the moment that this 1-D, Markov model correctly describes the flaring process. How do we interpret this result in terms of solar physics?

First, whatever the physical nature of the individual sites, the preferred limit $p_{re} \rightarrow 1$ implies they must be able to 'recharge' on times short compared to flare durations. This probably favours scenarios in which they are essentially microscopic in nature (e.g. double layers - Haerendel, 1994), rather than macroscopic (e.g. formation of nulls or current concentrations in response to evolving boundary conditions).

Second, the system must have some way of avoiding values of $p_1 > p_c$. In the limit $p_{re} \rightarrow 1$, $p_c = 0.74$ (Paper II). (Local) values of p_1 are intrinsic parameters and cannot, at first sight, be influenced by extrinsic, indeed emergent parameters such as the value of p_c . If the Sun were indeed free to pick any value of p_1 at random, roughly one flare in four would be 'infinite' in size - in practise, presumably, comparable to the largest flares ever seen. Clearly this is not the case, so how physically do we avoid $p_1 > p_c$?

Imagine driving an initially simple magnetic configuration with flux emergence and random velocity fields. As the total energy of the system increases, so also will the likelihood of individual energy release sites flaring. Occurrence of such an event and the consequent energy release 'avalanche' in turn reduces the total stored energy and also the likelihood of further sites spontaneously flaring. Thus it is physically reasonable that the total stored energy and the value of p_1 will be correlated. The occurrence of larger and larger flares as the system is driven towards p_c will then act as a feedback mechanism ensuring we always have $p_1 < p_c$. The approach of Wheatland & Glukhov (1998) offers a starting point for development of this idea, which naturally avoids any unobserved correlation between event sizes and time intervals between flares (see Biesecker 1994; Crosby 1996; Crosby et al. 1998; and also Rosner & Vaiana 1978, and Lu 1995c).

These ideas will be investigated further elsewhere (note also that A Conway, private communication, has constructed an analytical description of the appropriate generalisation of Paper I). In the present work we proceed by arbitrarily restricting $p_1 < p_c$, noting the potential justification along the above lines.

3. CA model with extended connectivity/dimensionality

In Paper I we contended that extension into 2 or 3 dimensions might bring our initial simplistic model into greater harmony with observations, either separately or, more likely, in conjunction with allowing repeated activity of a site during an event. It might also be argued that for greater physical realism we would want to consider the model embedded in a 3-D geometry. It can easily be seen how the existing model operating on a 1-D

lattice can be imposed on a 3-D lattice with no changes in principle required although with obviously greater complexity as the number of immediate neighbours for each site on a cubic lattice increases from 2 to 6. We contend at this stage that the degree of inter-connectedness of sites will reflect field line topology - e.g. Lau (1993); Longcope (1996) - rather than the dimensionality of the underlying space, and so it is important to draw a distinction between the dimension of the lattice and the connectivity of sites within it. Results from percolation theory confirm this distinction as for 2-D triangular, square or honeycomb lattices the percolation threshold $p_c = 0.50000, 0.59275$ and 0.6962 respectively (e.g. Stauffer & Aharony 1994).

We have already raised this issue with respect to the SOC models of LH (MacKinnon & Macpherson 1997) where we considered the effect on the SOC state of introducing increased connectivity between elements in the simulation box and other remote (i.e. non-neighbouring) elements. Our results indicated that the degree of connectivity imposed on the simulation could strongly influence the resulting SOC state, and indeed its whole stability.

The recent study by Litvinenko (1998) has produced analytical asymptotic estimates for the power-law index of the event size distribution of our model as outlined in Paper II. These are obtained in the limit where the number of active sites at any given time is small compared with the total number of sites. Additional results are also obtained for the upper energy cut-off and p_c . These results estimate the power-law index for the total event size (energy) distribution as $\alpha_E = 1.5$, *independent of dimensionality*. Previously, Wheatland & Sturrock (1996) had demonstrated the dependence of the distribution power-law indices predicted by the LH-type models on their dimensionality. This raises concern as one would expect the dimensionality to be determined by the complexity of the coronal magnetic field which can vary considerably during the solar cycle. Only small periodic changes in the power-law indices have, however, been discovered (Bai 1993) and thus the independence of the analytical estimate of α_E on the dimensionality within our model construction could be an important element in our model's favour (Litvinenko 1998).

The numerical simulations of the present work allow comparison with some of the asymptotic estimates derived by Litvinenko (1998). In Sect. 2, we demonstrated the effect which changing p_{re} has on the results. Indeed, we have shown that in 1-D, large values of p_{re} produce in themselves an excellent agreement with observations. We do not wish therefore to repeat all these simulations in 3-D in such depth but to concentrate mainly on trying to establish specifically the effect that changing the geometry has on the model results. Combining changes in geometry with inclusion of the full spectrum of recharging timescales follows naturally thereafter. Hence the discussion here is limited principally to the specific case (a) $p_{re} = 1$, recharging after exactly one inactive timestep, with several subtypes also discussed. For comparison we also briefly consider case (b) $p_{re} = 0$, equivalent to the formulation of Paper I and case (c) where sites can remain active for 2 or more consecutive timesteps.

3.1. Implementation and results

Following the same evolution laws as set out in Paper I and restated in Sect. 2 above, we simulate our CA on a 50^3 3-D grid counting 6 neighbours. Thus any one site can now have a possible 6 active neighbours in the previous timestep, rather than a maximum of 2. We consider only one triggering probability p_1 , indicating an enhanced flaring probability conditional on at least one active neighbour in the previous timestep, rather than introducing different triggering probabilities depending on the number of active neighbours. (A similar simplification was carried out in Paper II.)

We consider case (a) in detail first. Carrying out a simulation of expected event size as a function of stimulated probability p_1 (cf Fig. 1 for 1-D), indicates a divergence threshold of $p_c \approx 0.22$. More detailed numerical simulation is required to produce a precise value for p_c and as we show becomes vital to establish the exact power-law distributions in 3-D. For a single, fixed value of p_1 , the considerably enhanced complexity of the system now means that it is not possible to obtain an analytical expression of any kind for either $P(N)$ or $\langle N \rangle$. However, attempts to generalise the argument leading to Eqs. (1) and (2) lead to a qualitative expression of the form

$$P(N) = \eta(N)p^N(1-p)^{\kappa(N)} \quad (4)$$

which, of course, has too much functional freedom to be useful, but provides a useful framework for discussion. Here $\eta(N)$ has the same significance as previously, and $\kappa(N)$ is essentially the number of non-flaring sites surrounding the boundary of the cluster. $\eta(N)$ and $\kappa(N)$ are monotonically increasing functions of event size N . Litvinenko's (1998) discussion concentrates on $\eta(N)$. We see that $\eta(N)$ increasing more slowly than exponential leads to a drop-off in $P(N)$ from a power-law form at high N . This is what we see clearly in Eq. (2). Since we cannot prove analytically that $\eta(N)$ does not increase exponentially in the 3-D geometry, we consider a few Monte-Carlo simulations in which we derive total energy distributions for specific values of $p_1 < p_c = 0.12, 0.15$ and 0.18 (chosen to provide a broad sample of results below the threshold). The results of these simulations are shown in Fig. 2. A fall-off at high event sizes is observed in each case, long before possible finite-grid size effects or other numerical limiting factors can take effect. Hence we show the need to average over p_1 below p_c , as was necessary in the 1-D, reflaring case.

We note that in Fig. 2, and also in Figs. 3–5, the y-axis (number of events) includes values less than 1. This is because the method of "variable gridding" (M. Georgoulis, private communication) has been used, to avoid loss of statistical information. This method essentially weights the occurrence of one event of size 5000 say differently from one of size 50000 as the latter would be binned within a larger bin size. This produces weighted values for large events which are potentially less than 1, but allows extension of the frequency distribution over additional orders of magnitude.

As expected, when we average over p_1 the system exhibits strong power-law behaviour. For the specific case of $p_{re} = 1$

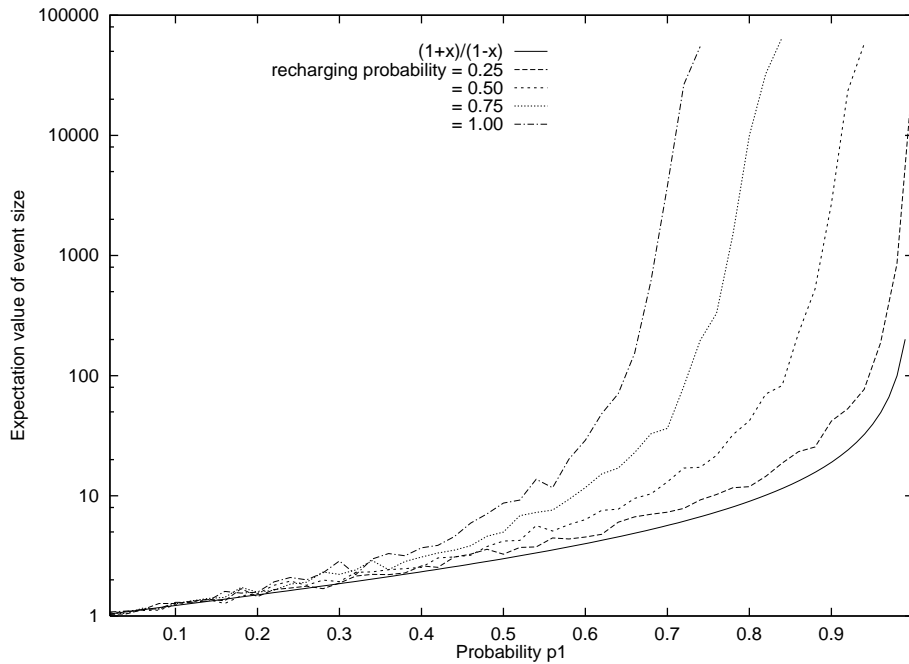


Fig. 1. Event size expectation value as a function of p_1 , parametrised by different values of the recharging probability p_{re} . The limiting case $p_{re} = 0$ is shown for reference. Note that this graph is on log-linear scaling. (Reprinted from *Physica A*, 243, Macpherson & MacKinnon, One-dimensional percolation models of transient phenomena, p1, ©1997, with permission from Elsevier Science.)

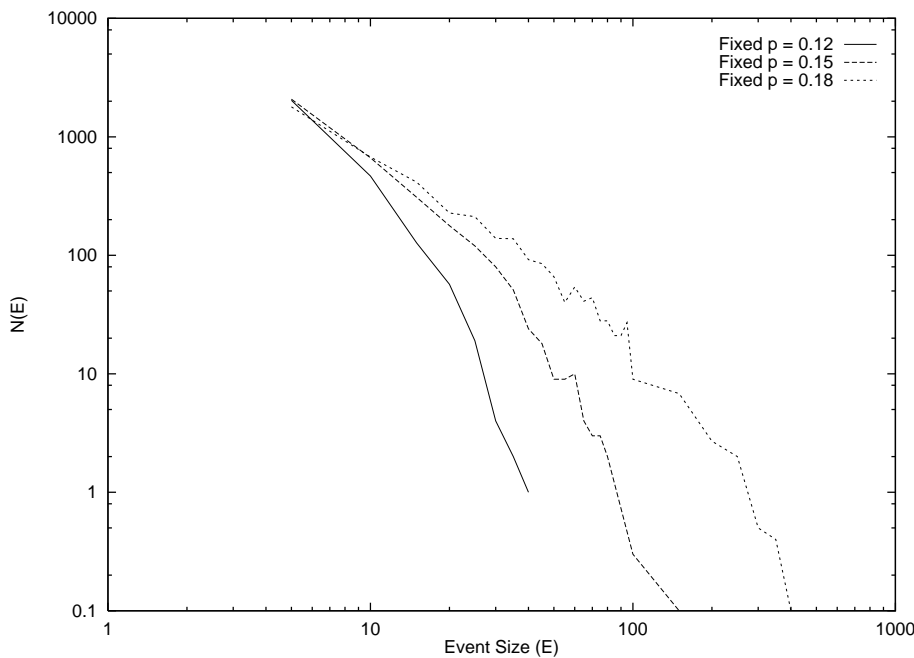


Fig. 2. For a fixed value of p_1 , we see that the event size distribution shows a strong fall-off from power-law behaviour as we get to larger event sizes. This confirms the need to average over p_1 below p_c , as was necessary in the 1-D case.

in 3-D we find a power-law index for the total energy distribution of $\alpha_E = -1.76 \pm 0.04$ (see Table 1 - case (a)). This is slightly steeper than observed, with α_E typically $\approx -1.5, -1.6$. The total energy frequency distribution for case (a) is shown in Fig. 3. Table 1 lets us compare these results with case (b), no reflaring. We expect that the frequency distributions should be steeper as there are more restrictions on generating very large events. This is true for α_E although not significantly statistically. The reason why allowing reflaring does not appear to influence the power-law indices as significantly as in 1-D is due to the comparative lack of accuracy with which we have calculated the threshold values p_c and also to the artificial upper cut-off

which we have imposed on the event size in order to make the numerical simulations more tractable. With respect to the first point, we show in Table 1 sub-types (a)-I, II and III the effect of artificially changing the threshold value. This causes significant changes in α_E (and also α_P and α_D) for small changes in p_c and demonstrates that in 3-D particularly we need more than 2 decimal place accuracy in calculating thresholds if we are to establish the precise power-law indices generated in each case (cf Stauffer & Aharony 1994 which quotes 5 decimal places as the determined p_c values for different 2-D lattices). In addition, imposing the upper limit on event size within the numerical scheme means that some large, long duration events are

Table 1. This table gives the power-law indices for the total energy, peak flux and duration distributions for different cases of our cellular automaton in 3-D. The different cases are described in detail in the text. For (a)-III, no error bar is included for α_P as it is statistically meaningless.

Case	p_{re}	p_c	α_E	α_P	α_D
(a)	1	~ 0.22	-1.76 ± 0.04	-2.69 ± 0.17	-2.10 ± 0.08
(a)-I	1	0.20	-1.92 ± 0.05	-3.58 ± 0.54	-2.65 ± 0.09
(a)-II	1	0.18	-2.53 ± 0.07	-4.59 ± 0.41	-3.11 ± 0.15
(a)-III	1	0.15	-2.87 ± 0.23	-7.07	-4.05 ± 0.20
(b)	0	~ 0.25	-1.81 ± 0.04	-2.35 ± 0.17	-2.27 ± 0.11
(c)	-	~ 0.21	-1.62 ± 0.05	-2.45 ± 0.16	-2.16 ± 0.08

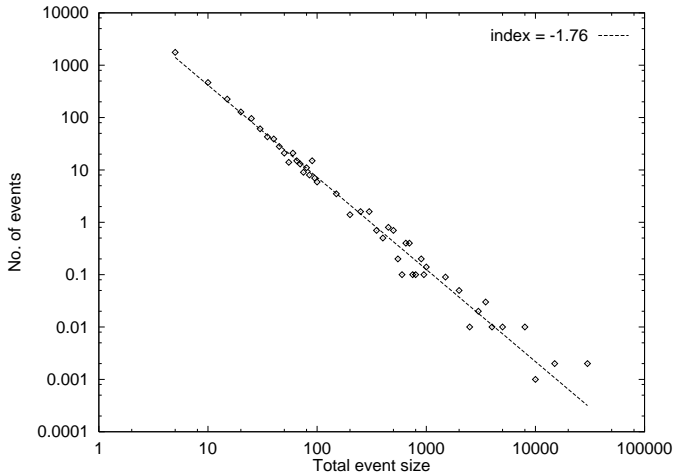


Fig. 3. The 3-D CA simulation still shows strong power-law behaviour in the frequency distributions for total event size, the precise index depending on the recharging timescale and the accuracy of the calculated divergence threshold.

mistakenly classified as effectively infinite, thus affecting the frequency distribution. Proper consideration of both those effects through much more extensive numerical simulations will provide more accurate values for the power-law indices. These are anticipated to be slightly lower than the ones quoted here, for the reasons just given, and thus also closer to the estimates of Litvinenko (1998).

Besides the numerical effects just described, there are other factors which we discarded earlier which can be relaxed to provide a wider range of power-law indices. First of all, assuming that the stimulated probability is the same irrespective of how many neighbours are active reduces the combinatorial complexity of the model, and allows us to write down Eq. (4). Furthermore, it is possible also to introduce a probability that any active site can remain active for more than one consecutive timestep - see also Paper II. In this case, we do not require that a site is necessarily switched off following activity, but instead may remain active under the probability of stimulated flaring from a neighbouring active site. Case (c) in Table 1 demonstrates the reduction in α_E which can be achieved by allowing this scenario, producing a power-law index in close agreement with observa-

tions. We may argue that we have physical grounds for desiring that an active element becomes inactive following triggering. Recharging could potentially take place on a shorter timescale than energy release, however, and a discrete simulation with a resolution of one timestep does not allow for fractionation of these timescales. Therefore we consider case (c) as a potential limiting example.

Taking these factors into consideration, we can confidently assert that the model can provide a quantitative match to observed total flare energy distributions while demonstrating the great degree of flexibility in the results depending on which assumptions regarding the connectivity and recharging timescales are adhered to. Specifically, cases with rapid recharging, or in which sites remain active for longer than a ‘stimulated flaring time’, are preferred. This is true even with a 3-D model.

3.2. Peak flux and duration power-law frequency distributions

The works of LH, Lu et al. (1993) and Vlahos et al. (1995) also consider fits to the peak event size and event duration frequency distributions, also observed to exhibit strong power-law behaviour for solar flares. In 1-D, while the total energy distribution has been well matched by our CA model, there is limited scope for reproducing also these other distributions. Thus a 3-D geometry may allow us to compare our model more closely with the self-organising avalanche models, and has the potential for greater agreement with observations. The peak size (flux) and duration frequency distribution power-law indices are referred to as α_P and α_D respectively. Table 1 therefore also lists the relevant power-law indices for the peak flux and duration distributions for the different cases studied. The duration distribution is well fit by a power-law in each case, over about two orders of magnitude (see Fig. 4 for case (a)), with a power-law index of -2.10 ± 0.08 for case (a). The most that can be claimed for the observed duration distribution is a power-law over about one order of magnitude (Crosby et al. 1993; Bromund et al. 1995; Crosby 1996). Crosby et al. (1993) calculates the frequency distribution for SMM HXRBS data and finds a power-law index which varies between -1.95 and -2.22 , depending on which subinterval of SMM observing time is considered. Within these parameters, our model results fit the observations very well.

The peak flux distribution is much steeper than is observed (α_P observed ~ 1.7 – 1.8 depending on which database is used, Dennis, 1985; Crosby et al. 1993; Biesecker 1994; Crosby 1996), see Fig. 5 for the frequency distribution, again for case (a). In the cases (a)-I, II and III, the distributions exist only up to a maximum of one order of magnitude, and hence the number of points included in the fit, using the variable gridding method, is less than 10. This results in the noticeably larger deviations quoted for cases I and II. Indeed for case III the deviation is statistically meaningless and so not quoted. The exact values are not the most crucial elements, the trend with decreasing p_c and the steeper-than-observed distributions are the important features. In particular, the range of values is, however, in closer agreement with the type of steeper peak flux frequency distribution discussed by Vlahos et al. (1995), Georgoulis &

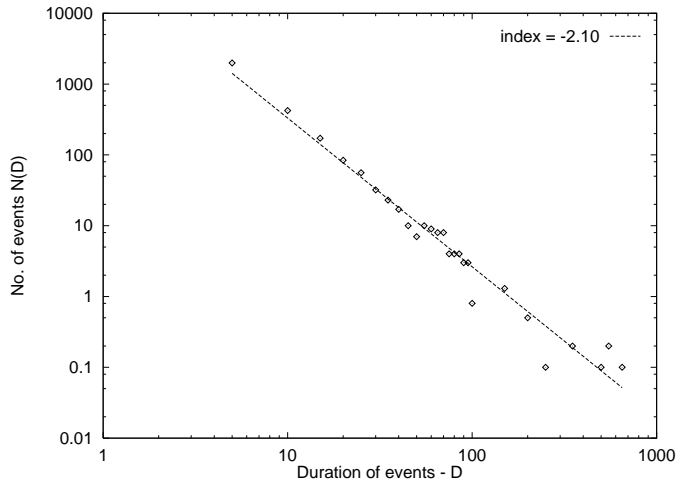


Fig. 4. Strong power-law frequency distribution for event duration is observed in case (a) for the 3-D CA simulation.

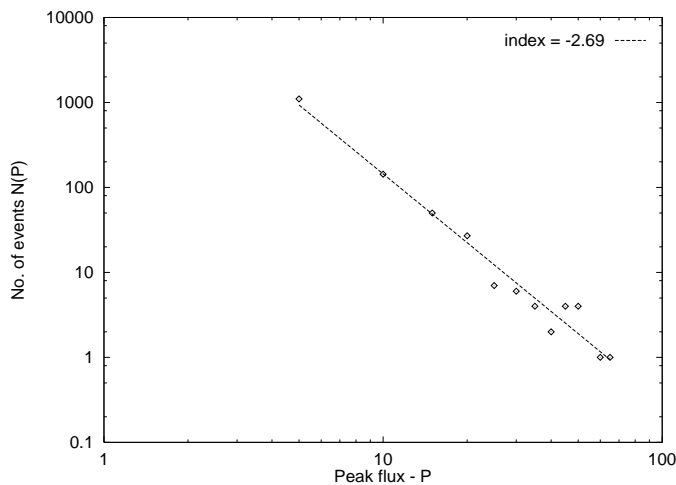


Fig. 5. A power-law frequency distribution for event peak activity is observed in case (a) for the 3-D CA simulation, although only over about one order of magnitude.

Vlahos (1996, 1998) when they introduce an anisotropic instability criterion. In the original LH model, the instability criterion in their 3-D simulation is based on an isotropic average over the 6 nearest neighbours on the lattice. In contrast, the anisotropic criterion includes instabilities when they occur between any 2 neighbouring sites on the lattice. They find that this construction produces as a result much steeper values of α_P , although the distribution extends only over an order of magnitude at most (Georgoulis & Vlahos 1996, 1998). These authors have calculated that the steeper peak flux frequency distribution which arises in their model from anisotropic, or independent, triggering contains most of the total energy released by the system. They therefore propose that this steeper distribution of “nanoflares” could still play an important role in heating the corona - although the existence of such a distribution remains to be confirmed unequivocally by observations.

The results of Georgoulis & Vlahos (1996, 1998) are directly analogous to the present findings, in that the peak flux

frequency distribution only exists over about an order of magnitude. (Observations show up typically 3 orders of magnitude for the distribution). Our model construction is such that the 6 neighbours around any active site are independent in their triggering, relying only on the stimulating probability. In the next section, by comparing the construction of our model with ‘standard’ SOC models, we give reasons why we conclude that this independence in allowing the neighbouring sites to be triggered by one active site manifests itself in the steepness of the peak flux frequency distribution. Consequently, the isotropic instability criterion of LH is an essential feature of their construction in fitting the observed peak flux frequency distribution.

We note that this discussion pre-supposes the hard X-ray flux to reflect directly the time development of the energy release process - which need not be the case.

4. Comparison with SOC models

Above we saw that our approach can succeed in reproducing flare size and duration distributions, but that our peak intensity distributions are steeper than those observed. On the other hand, LH *et seq* have been able to reproduce adequately the distributions of all three of these quantities. In this section we re-examine the LH approach, showing formally how parameters like our probabilities for spontaneous and stimulated flaring might be calculated from its basic assumptions. The discussion will have the character of an existence proof, not calculating these quantities in particular cases, but demonstrating that they may be calculated. This process: clearly establishes the parallels between our formal approach and the more physically motivated LH one; isolates those attributes of the LH procedure which are responsible for its various successes; and points the way towards more general, formal models of the sort introduced in Papers I and II, and here, that would subsume both the present approach and that of LH.

LH studied a system introduced, by analogy with sandpile or earthquake models (Bak et al., 1987, 1988), as an analogue for the relaxation of a complex, driven magnetic field. At each point (i, j, k) of a 3-D lattice, there is a quantity $V_{i,j,k}$ which is variously scalar- (e.g. Vlahos et al. 1995) or vector-valued (e.g. LH, Lu et al. 1993). In what follows we deal only with a scalar V , although it will be clear that no vital new feature emerges if V is vector-valued.

Consider first how the models are driven, i.e. how a single site in each model first attains the ‘flaring’ state. In the LH approach, initial values are assigned to all V . At each time $t > 0$, a random quantity, drawn from a time-independent distribution with non-zero mean, is added to a randomly chosen site. This quantity represents the external driving of the system so its distribution does not depend on any $V_{i,j,k}$. At each (i, j, k) , define the gradient function as a weighted average of $V_{i,j,k}$ and its 6 rectangular neighbours (V_f):

$$D_{i,j,k} = V_{i,j,k} - \frac{1}{6} \sum_f V_f \quad (5)$$

where \mathbf{f} takes the values $(i \pm 1, j, k)$, $(i, j \pm 1, k)$ and $(i, j, k \pm 1)$ in the summation. Random incrementing of the $V_{i,j,k}$ continues until some $D_{i,j,k} > D_{th}$, a threshold value, whose exact value is unimportant for the behaviour of the model (Lu et al., 1993; MacKinnon & Macpherson, 1997). Different, deterministic evolution rules are then followed until the resulting ‘flare’ comes to a stop, after which the random incrementing process begins anew from the new set of initial values determined by the outcome of applying these rules (Presumably the ‘timestep’ has quite different physical significances during these two distinct modes).

Random incrementing of the $V_{i,j,k}$ in this way essentially generates a distribution of values of these quantities, whose exact form is determined by the distribution from which the increments are drawn. For example, random increments drawn from a Wiener process with zero mean generate a Gaussian distribution whose variance increases linearly with time (e.g. Gardiner, 1985). Thus, at time δt after the last flare, the value of $V_{i,j,k}$ may be written

$$V_{i,j,k} = V_{i,j,k}^0 + \delta V \quad (6)$$

where $V_{i,j,k}^0$ was the value of $V_{i,j,k}$ at the end of the last ‘flare’ and δV is a random quantity whose distribution depends only on δt . $D_{i,j,k}$ can similarly be written

$$D_{i,j,k} = D_{i,j,k}^0 + \delta D \quad (7)$$

where $D_{i,j,k}^0$ and δD are simply given by the appropriate weighted averages. Again, the distribution of δD depends only on δt .

For given $D_{i,j,k}^0$, then, the average time interval until the next flare is given by the solution of the ‘first crossing time’ problem implied by Eq. (7) and the condition $D_{i,j,k} > D_{th}$. In the SOC state, the distribution of ‘post-flare’ initial values $D_{i,j,k}^0$ will also be time-independent and thus we can in principle calculate a single, time-independent probability p_0 of ‘flaring’ at any site, given by averaging the result of the first crossing problem for particular $D_{i,j,k}^0$ over the distribution of values of this quantity which characterises the SOC state. In the present work this number is regarded as a parameter, and in the LH approach it is calculated numerically, as described, from underlying probabilistic assumptions, but the net result is the same.

Consider now what happens once the threshold condition is satisfied at some (i, j, k) . The values of $V_{i,j,k}$ and its six nearest neighbours ($V_{\mathbf{f}}$) are evolved in a way which reduces the gradient:

$$V_{i,j,k} \rightarrow V_{i,j,k} - \frac{6}{7} D_{th}, \quad V_{\mathbf{f}} \rightarrow V_{\mathbf{f}} + \frac{1}{7} D_{th} \quad (8)$$

Now we ask, what is the probability that any of the neighbouring sites is unstable as a result of this redistribution? To be concrete, we consider site $(i + 1, j, k)$, although the discussion will clearly hold for any of the neighbours. We need to consider the probability that

$$D_{i+1,j,k} > D_{th} \quad (9)$$

Once again, the probability distribution of $D_{i+1,j,k}$ can be written in terms of the distributions of the values of V at

$(i + 1, j, k)$ and its six neighbours. All of these except $V_{i,j,k}$ and $V_{i+1,j,k}$ still have the values they had when (i, j, k) first became unstable, i.e. those given in a time-independent way by the convolution of Eq. (6) with the distribution of time intervals between flares. Site (i, j, k) itself, however, has been readjusted in such a way as to reduce $D_{i,j,k}$ below D_{th} , so its value is now a representative of the immediate post-flare distribution, and the distribution of its values is the immediate post-flare one. Also, $V_{i+1,j,k}$ has had added to it a quantity drawn from a distribution which is again, in principle calculable, and very simply related to the distribution of values of sites $V_{i,j,k}$ when they become unstable. Thus, again, we can determine the probability that Eq. (9) is satisfied from a linear combination of quantities with known distributions. These distributions are all time-independent, but they are different, because the operations in Eq. (8) have been carried out, from the distributions that determine flare onset. Thus the probability of a neighbour of a ‘flaring site’ becoming unstable in consequence can be represented, once again, by a single, time-independent probability, just as in the present work. With the parallels between our approaches clarified in this way, below we discuss further features of the LH approach in our own language.

An ‘energy’ released by each re-adjustment is calculated from the changes in V . Again, this function of the values of the various V will have a well-defined probability distribution function. Unless this distribution function has a large standard deviation, and/or a long, non-Gaussian tail, it will contribute only slight changes to the flare ‘size’ distribution, compared to that obtained by simply counting the number of unstable sites during the flare.

As a flare progresses, sites may find that more than one of their neighbours have flared in the previous timestep. Then more than one of the neighbours will be representatives of the immediate post-flare values V^0 , and the probability of stimulated flaring of a site will depend on the number of flaring neighbours. We have mentioned this possibility previously in Papers I and II and explored it to some degree, finding that it introduces no qualitatively new features - although see the discussion below on matching the peak flux frequency distribution.

In the LH approach, individual sites may become unstable more than once during a single flare. The probability of such an event will be different from that of stimulated flaring, because the unstable site is now a representative of the post-flare values V^0 . This distinction is mimicked (though not, apparently, duplicated) by the introduction (Paper II and Sect. 2 in this work) of the ‘reflaring probability’.

Consider now the probability, following a single site becoming unstable, that two of its neighbours also become unstable in the next timestep. In the formalism of this paper this is just p^2 , because the events are independent. In the LH approach, however, both sites must satisfy criteria like Eq. (9), both of which involve the value of $V_{i,j,k}$. Thus the probabilities are not independent, and we cannot get the probability of both becoming unstable simply from their separate values. This is the key distinction between LH and our approach, and this is the factor

that allows large events to grow rapidly, leading in particular to greater peak fluxes.

This distinction between the models becomes clear if we further compare our model with the anisotropic instability criterion of Georgoulis & Vlahos (1996, 1998), as alluded to in the previous section. This criterion generates a ‘nanoflare’ distribution with a steeper power-law index because an instability between two individual sites is more likely than one averaged over six rectangular neighbours. Furthermore, in the isotropic case, the redistribution laws as given by Eq. (8) show that one unstable point subsequently affects all six neighbours and can therefore trigger instabilities in some or indeed all of them; in the anisotropic case only the neighbours involved in the instability are affected by the redistribution, and thus the event does not have the same potential to grow and spread rapidly. Combined these effects produce the steeper nanoflare distribution.

The same effects naturally produce the same results in our model as the independence of stimulated flaring means that one flaring site triggers n other sites in the next timestep with probability p^n , which obviously decreases rapidly as we increase n , greatly lowering the probability of one site triggering all six neighbouring sites. Additionally, in parallel with the approach of Georgoulis & Vlahos, by not introducing separate probabilities p_2, p_3 etc for 2, 3, ... neighbours being active, we have removed the possibility of a site being stimulated twice or more by 2 or more active sites, unlike in LH where a site can receive an additional $\frac{1}{7}D_{th}$ for each unstable neighbouring site (from Eq. (8)).

Developing our model to account for these differences from the LH approach is one obvious next step. We do not, however, pursue this further here. Instead we reiterate that one strong conclusion of our work is that the isotropic instability criterion of the LH model construction is a key factor in their success in fitting the peak flux frequency distribution, in addition to the total energy and duration distributions. Moreover, it indicates that more sophisticated, physical modelling will also need such a feature to be similarly successful.

5. Discussion and conclusions

One might hope that the distribution of flare sizes would be a vital clue to the physical nature of an individual flare process. However, the realisation that it may be an *emergent* property of the ensemble of elementary energy release processes carries with it a discomfiting corollary: this flare size distribution on its own does not allow us to discriminate between rival theories for the nature of these elementary events. All that it may allow us to deduce, via comparison with models of the sort described here, is the degree of interconnectedness of the elementary events, and the relative magnitudes of the driving and relaxation timescales. The relevant physics therefore becomes that of statistical properties of a self-organising system, rather than the physics of one specific energy release event. While a particular physical picture may satisfy the necessary requirements of connectedness, it will be harder to argue that it does so uniquely.

The picture of LH, for example, was introduced originally as a sort of analogue for the guessed behaviour of locally reconnecting magnetic fields in a system driven by photospheric turbulence; Zirker & Cleveland (1993) developed an avalanche model based on the twisting and/or braiding of coronal magnetic field lines; Litvinenko (1994, 1996) proposed the interaction through coalescence of reconnecting current sheets while Wheatland & Glukhov (1998) generalise the stochastic flare model of Rosner & Vaiana (1978). All of these models reproduce power-law frequency distributions for flare parameters, but the reverse engineering of the details of their individual constructions from the final distributions obtained is clearly not possible.

The aim of this work has been to propose that the common thread running through these different proposals is the way in which the different elementary release processes are allowed to interact and it is in this area that we may hope that the range of flare frequency distribution parameters will allow us to draw conclusions and to place general constraints. We envision that some additional alternative picture involving, for instance, multiple double layer formation (Haerendel, 1994), but in which the elementary events were able to communicate with the same degree of inter-connectedness as one of the alternative models described above, would produce very similar event size distributions.

We have previously emphasised (Paper I; MacKinnon & Macpherson, 1997) that neither the underlying 3-dimensional space, nor the topology of the field, may totally determine this degree of interconnectedness. Thus, in parallel with studies of field line topology (e.g. Lau 1993; Longcope 1996), the sort of parametric study carried out here enables the only sort of model-independent deductions one can honestly make from event size data.

The stochastic model which we have outlined attempts to capture and explain some of the ways in which we may understand the scale invariant behaviour observed. Building on a simplistic analytical 1-D model which provided only a qualitative fit to the observed flare total energy frequency distribution, we have parameterised the reflaring probability of individual energy release sites within the lattice, in line with observations showing repeated local energy release throughout the duration of a flare. In particular in Sect. 2 we have shown how the best fits with observations are obtained if individual sites recharge in timescales much less than flare durations. The convergence of the numerical simulations of our model to produce a total energy power-law index of 1.5 is in agreement with the recent analytical estimates obtained by Litvinenko (1998).

Embedding our model in a 3-D space is not predicted to make considerable changes to the total energy power-law index as the asymptotic estimate for this is independent of dimension (Litvinenko 1998). This is confirmed by the results obtained although considerably greater numerical effects do come into play and further dedicated numerical simulations will be necessary to establish the divergence thresholds in 3-D and the degree to which the numerical simulations match up with the analytical scalings proposed by Litvinenko (1998). Extension to 3-D

also allows discussion of the frequency distributions for event duration and peak event size. As shown in Sect. 3.2, the event duration distribution obtained provides a good fit with the observations as analysed by e.g. Crosby et al. (1993). The peak flux distribution does not match flare observations exactly, tending to be steeper than actually observed. How seriously we take this failure depends on how confident we are that hard X-rays directly reflect the energy release rate. Duration and peak flux distributions for soft X-rays, for instance, are presumably influenced as much by the thermal response of the flare plasma as by details of the primary energy release rate; and fast electron transport, involving electron propagation and trapping times (e.g. Aschwanden et al., 1998) will similarly complicate these quantities' distributions for the hard X-ray case. The extreme case of long-duration hard X-ray events, well interpreted in terms of coronal electron trapping (Bai & Ramaty 1979; Vilmer et al. 1982) surely sounds a warning. While other models' successes in this regard are interesting, they might only be coincidental; and we need to remember that even (optical) event size distributions for other stars (e.g. Gershberg & Shakhovskaya, 1983) are, apparently, not always well fit by SOC models, suggesting that luck may play a part in their success in the solar case.

Even if we take this difficulty seriously, however, it serves a useful purpose: that of highlighting the ingredient of LH type models that makes them successful in this respect, and thus, in general terms, the attribute which more physically detailed models must have in order to share this success. Georgoulis & Vlahos (1996, 1998) obtain similarly steep peak flux distributions in LH SOC type simulations with an anisotropic instability criterion, in which instabilities trigger independently between nearest neighbours. Since the lattice sites in our stochastic model are also independently triggered, this close analogy in behaviour with our general construction shows one property of the interaction of sites required to fit the peak flux distribution observations – namely that the probabilities of individual neighbours flaring should not be independent. Georgoulis & Vlahos (1996, 1998) associate their steeper distributions of small events with nanoflares, although these have still to be observed unequivocally and their frequency distribution established.

The extent to which the redistribution laws of the SOC models actually mimic 3-D reconnection is still uncertain, although two companion papers by Isliker et al. (1998) and Vassiliadis et al. (1998) have sought to show how the solar flare SOC constructions of the type discussed in LH, Lu et al. (1993) and Vlahos et al. (1995) can be recast from or interpreted as discretized magnetohydrodynamic (MHD) equations. Numerical MHD simulations of the behaviour of a coronal loop subjected to random magnetic forcing (Einaudi et al. 1996; Galsgaard & Nordlund, 1996; Georgoulis et al. 1998) have demonstrated that the energy dissipation in the system is intermittent, and that the spatiotemporal evolution can be statistically described in terms of power-law distributions for total energy, peak activity and duration of events (see also Dmitruk & Gómez 1997; Galtier & Pouquet 1998). Indeed, following up the comments on reverse engineering, given a power-law distribution of flare parameters, it would be difficult to determine whether it was pro-

duced through a discrete lattice grid or continuous MHD driven simulation – however, as we have aimed to show here, general constraints on the topology, timescales and spatial dimensions may be derivable.

In the recent years since the publication of the first avalanche models of solar flaring, several new pieces of observational evidence have been obtained which emphasise the fragmented nature of energy release during flares and thus strongly support this picture (see Bastian & Vlahos 1997 and references therein - also van den Oord 1994 for the proceedings of a workshop dedicated to the issue of fragmented energy release). In particular, higher resolution observations of solar flare occurrence have demonstrated the continuation of the scale invariant power-law distributions observed by SMM and earlier. In addition Kucera et al. (1997) have provided evidence for a cutoff in the frequency distribution of flares from small active regions, a result which they claim is consistent with the predictions of the avalanche model of Lu (1995a, b). Furthermore, modelling of active region development through percolation models of emerging magnetic flux have shown that complex systems methods are increasingly applicable to studying solar behaviour (e.g. Wentzel & Seiden 1992; Seiden & Wentzel 1996; Mylonas et al. 1998).

In conclusion, we have aimed to show that the statistical properties of the model, i.e. the size distribution, etc are determined by the dimensionality and spatial form of the lattice together with the transition probabilities. Insisting on models which agree in their statistical properties with observations then restricts the degree of inter-connectedness of elementary flare sites, and the relative magnitudes of their energy storage and release timescales. *Once we agree that the observed event size distribution results from the self-organisation of elementary processes, the quantities determining how these processes self-organise are the only quantities we may hope to deduce from that distribution.* Only if a theory for the physical nature of the elementary energy releases also inevitably prescribes their degree of inter-connectedness, can such physical hypotheses be borne out by this sort of argument.

Acknowledgements. KPM's contribution to this work was started as a PDRA in the Department of Physics & Astronomy of the University of Glasgow, under PPARC Grant 4071BW, and finished as a PDRA at the University of Oxford under Grants GR/K46224 and PPA/G/S/1997/00279. The numerical simulations were carried out on the STARLINK computer facilities at the University of Glasgow. The authors would like to thank the anonymous referee for suggestions to improve the overall quality of the paper.

References

- Aschwanden M.J., Schwartz R.A., Dennis B.R., 1998, ApJ 502, 468
- Bai T., 1993, ApJ 404, 805
- Bai T., Ramaty R., 1979, ApJ 227, 1072
- Bak P., Tang C., Wiesenfeld K., 1987, Phys. Rev. Lett. 59, 381
- Bak P., Tang C., Wiesenfeld K., 1988, Phys. Rev. A 38, 364
- Bastian T.S., 1991, ApJ 370, L49
- Bastian T.S., Vlahos L., 1997, In: Trotter G. (ed.) Coronal Physics from Radio and Space Observations. Lecture Notes in Physics, Springer Verlag, 68

- Berghmans D., Clette F., Moses D., 1998, *A&A* 336, 1039
- Biesecker D.A., 1994, Ph.D. Thesis, University of New Hampshire
- Bromund K.R., McTiernan J.M., Kane S.R., 1995, *ApJ* 455, 733
- Carlson J.M., Langer J.S., 1989, *Phys. Rev. Lett.* 62, 2632
- Crosby N.B., 1996, Ph.D. Thesis, Observatoire de Meudon, France
- Crosby N.B., Aschwanden M.J., Dennis B.R., 1993, *Solar Phys.* 143, 275
- Crosby N.B., Vilmer N., Lund N., Sunyaev R., 1998, *A&A* 334, 299
- Dennis B.R., 1985, *Solar Phys.* 100, 465
- Dmitruk P., Gómez D.O., 1997, *ApJ* 484, L83
- Einaudi G., Velli M., Politano H., Pouquet A., 1996, *ApJ* 457, L113
- Galsgaard K., 1996, *A&A* 315, 312
- Galsgaard K., Nordlund A., 1996, *JGR* 101, 13445
- Galtier G., Pouquet A., 1998, *Solar Phys.* 179, 141
- Gardiner C.W., 1985, *Handbook of Stochastic Methods*. Springer, Berlin-Heidelberg-New York
- Gary D.E., Hartl M.D., Shimizu T., 1997, *ApJ* 477, 958
- Georgoulis M., Vlahos L., 1996, *ApJ* 469, L135
- Georgoulis M., Vlahos L., 1998, *A&A* 336, 721
- Georgoulis M., Velli M., Einaudi G., 1998, *ApJ* 497, 957
- Gershberg R.E., Shakhovskaya N.I., 1983, *Ap&SS* 95, 235
- Gopalswamy N., Payne T.E.W., Schmahl E.J., et al., 1994, 437, 522
- Haerendel G., 1994, *ApJS* 90, 765
- Islaker H., Anastasiadis A., Vassiliadis D., Vlahos L., 1998, *A&A* 335, 371
- Krucker S., Benz A.O., 1998, *ApJ* 501, L213
- Kucera T.A., Dennis B., Schwartz R.A., Shaw D., 1997, *ApJ* 475, 338
- Lau Y.T., 1993, *Solar Phys.* 148, 301
- Lee T.T., Petrosian V., McTiernan J.M., 1993, *ApJ* 412, 401
- Lin R.P., Schwartz R.A., Kane S.R., Pelling R.M., Hurley C.C., 1984, *ApJ* 285, 421
- Litvinenko Y.E., 1994, *Solar Phys.* 151, 195
- Litvinenko Y.E., 1996, *Solar Phys.* 167, 321
- Litvinenko Y.E., 1998, *A&A* 339, L57
- Lockwood D.R., Lockwood J.A., 1997, *Complexity*, 2(4), 49
- Longcope D.W., 1996, *Solar Phys.* 169, 91
- Lu E.T., 1995a, *Phys. Rev. Lett.* 74, 2511
- Lu E.T., 1995b, *ApJ* 446, L109
- Lu E.T., 1995c, *ApJ* 447, 416
- Lu E.T., Hamilton R.J., 1991, *ApJ* 380, L89 (LH)
- Lu E.T., Hamilton R.J., McTiernan J.M., Bromund K.R., 1993, *ApJ* 412, 841
- MacKinnon A.L., 1986, In: Gondalekhar P.M. (ed.) *Flares: Solar and Stellar*. Rutherford Appleton Laboratory Workshop Proceedings RAL-86-085
- MacKinnon A.L., Macpherson K.P., 1997, *A&A* 326, 1228
- MacKinnon A.L., Macpherson K.P., Vlahos L., 1996, *A&A* 310, L9 (Paper I)
- Macpherson K.P., MacKinnon A.L., 1997, *Physica A* 243, 1 (Paper II)
- Mercier C., Trottet G., 1997, *ApJ* 474, L65
- Mylonas N., Vlahos L., Kluiving R., 1998, In: Alissandrakis C.E., Schmeider B. (eds.) *Second Advances in Solar Physics Euroconferences: Three-Dimensional Structure of Solar Active Regions*. ASP Conf. Ser. Vol. 155, 19
- Nagel K., Raschke E., 1992, *Physica A* 182, 519
- Porter J.G., Fontenla J.M., Simnett G.M., 1995, *ApJ* 438, 472
- Rosner R., Vaiana G., 1978, *ApJ* 222, 1140
- Seiden P.E., Wentzel D.G., 1996, *ApJ* 460, 522
- Shimizu T., 1995, *PASJ* 47, 251
- Shimizu T., Tsuneta S., Acton L.W., Lemen J.R., Uchida Y., 1992, *PASJ* 44, L147
- Stauffer D., Aharony A., 1994, *Introduction to Percolation Theory*. Rev. 2nd Ed., Taylor and Francis Ltd, London
- van den Oord G.H.J., 1994, In: van den Oord G.H.J. (ed.) *Fragmented Energy Release in Sun and Stars*. Kluwer, Dordrecht
- Vassiliadis D., Anastasiadis A., Georgoulis M., Vlahos L., 1998, *ApJ* 509, L53
- Vilmer N., Kane S.R., Trottet G., 1982, *A&A* 108, 306
- Vlahos L., Georgoulis M., Kluiving R., Paschos P., 1995, *A&A* 299, 897
- Wentzel D.G., Seiden P.E., 1992, *ApJ* 390, 280
- Wheatland M.S., Glukhov S., 1998, *ApJ* 494, 858
- Wheatland M.S., Sturrock P.A., 1996, *ApJ* 471, 1044
- White S.M., Kundu M.R., Shimizu T., Shibasaki K., Enome S., 1995, *ApJ* 450, 435
- Zirker J.B., Cleveland F.M., 1993, *Solar Phys.* 145, 119